ECOLE POLYTECHNIQUE

CENTRE DE MATHÉMATIQUES APPLIQUÉES
UMR CNRS 7641

91128 PALAISEAU CEDEX (FRANCE). Tél: 01 69 33 41 50. Fax: 01 69 33 30 11

http://www.cmap.polytechnique.fr/

A multiscale finite element method for numerical homogenization

Grégoire Allaire, Robert Brizzi

R.I. N^0 545 *July 2004*

A multiscale finite element method for numerical homogenization

Grégoire ALLAIRE
CMAP, UMR-CNRS 7641, Ecole Polytechnique 91128 Palaiseau Cedex (France)

Robert BRIZZI
CMAP, UMR-CNRS 7641, Ecole Polytechnique 91128 Palaiseau Cedex (France)

Abstract

This paper is concerned with a multiscale finite element method for numerically solving second order scalar elliptic boundary value problems with highly oscillating coefficients. In the spirit of previous other works, our method is based on the coupling of a coarse global mesh and of a fine local mesh, the latter one being used for computing independently an adapted finite element basis for the coarse mesh. The main new idea is the introduction of a composition rule, or change of variables, for the construction of this finite element basis. In particular, this allows for a simple treatment of high order finite element methods. We provide optimal error estimates in the case of periodically oscillating coefficients. We illustrate our method on various examples.

1 Introduction

The goal of this paper is to build a multiscale finite element for performing numerical homogenization. The word multiscale is understood here in the practical sense that two different meshes will be used: a fine mesh for computing locally and independently (i.e. allowing for an easy parallelization) a finite element basis, and a coarse mesh for computing globally and at low cost the solution of an elliptic partial differential equation. By numerical homogenization we mean that we compute, not only the mean field solution of a highly heterogeneous problem, but also the local fluctuations which may be important in many applications. Recently there has been many contributions on multiscale numerical methods, including [3], [6], [8], [9], [10], [11], [12], [13], [14]. Our work is in the spirit of that of Hou and Wu [11].

Our model problem is a scalar elliptic partial differential equation which arises in many applications such as diffusion in porous media, or composite materials. Let Ω be a bounded

open set of $\mathbb{R}^n$ and $f \in L^2(\Omega)$ (or, more generally, $f \in H^{-1}(\Omega)$). For simplicity, we consider Dirichlet boundary conditions. Our model problem is to find $u_\varepsilon \in H_0^1(\Omega)$ solution of

$$\left\{ \begin{array}{rcll} -\mathrm{div}\{A^\varepsilon \,\mathrm{grad}\, u^\varepsilon\} & = & f & \text{in } \Omega \\ \\ u^\varepsilon & = & 0 & \text{on } \partial\Omega \end{array} \right. \tag{1}$$

where $A^\varepsilon = (a_{ij}^\varepsilon)_{i,j=1}^n$ is a non-necessarily symmetric matrix of coefficients which all belong to $L^\infty(\Omega)$. We assume that A^ε is uniformly bounded and coercive. The notation $\varepsilon > 0$ stands for some small scale in the problem (but there could well be several scales, so ε is just a convenient notation for all the small scales of variation of A^ε). Solving numerically (1) is a difficult task if the scale ε is small. Indeed, a good approximation is obtained with classical finite element methods (or any other methods) only if the mesh size h is smaller than the finest scale, i.e. $h \ll \varepsilon$. As is well known, this is not satisfactory since CPU time as well as memory storage grow polynomially with h^{-1} and soon become prohibitively too large.

There is one way out of this difficulty in the special case of periodic heterogeneities or oscillations of the tensor A^ε. In the periodic case, ε is the period, and A^ε is defined by

$$A^\varepsilon(x) = A\left(\frac{x}{\varepsilon}\right),$$

where $y \to A(y)$ is a Y-periodic function where $Y = (0,1)^n$ is the unit cube. It is a classical result of homogenization theory (see e.g. [5]) that, for small ε, u^ε is approximated by

$$u^\varepsilon(x) \;\approx\; u^*(x) \;+\; \varepsilon \sum_{i=1}^n \chi_i\left(\frac{x}{\varepsilon}\right) \frac{\partial u^*}{\partial x_i}(x) \tag{2}$$

and

$$\nabla u^\varepsilon(x) \;\approx\; \nabla u^*(x) \;+\; \sum_{i=1}^n (\nabla_y \chi_i)\left(\frac{x}{\varepsilon}\right) \frac{\partial u^*}{\partial x_i}(x), \tag{3}$$

where χ_i is the solution of the so-called cell problem

$$\left\{ \begin{array}{rcll} -\mathrm{div}_y\{A(y)\left(e_i + \mathrm{grad}_y\, \chi_i\right)\} & = & 0 & \text{in } Y, \\ \\ y \;\to\; \chi_i(y) & & 0 & Y - \text{periodic}. \end{array} \right. \tag{4}$$

The numerical resolution of (1) is often replaced by the simpler one of the homogenized problem

$$\left\{ \begin{array}{rcll} -\mathrm{div}\{A^* \,\mathrm{grad}\, u^*\} & = & f & \text{in } \Omega \\ \\ u^* & = & 0 & \text{on } \partial\Omega. \end{array} \right. \tag{5}$$

where A^* is a constant homogenized tensor given by the explicit formula $A^* e_i = \int_Y A(y)\left(e_i + \mathrm{grad}_y\, \chi_i\right) dy$. The approximation of u^ε by u^* can be improved by adding the *first order corrector term* εu_1. This additional contribution may not be so important in (2) but is crucial in (3) since it is of the same order of magnitude than ∇u^*. Note in passing that (2) and (3) can also be improved by adding a so-called *boundary layer term* since $u^* + \varepsilon u_1$ does not satisfy the Dirichlet boundary condition on $\partial\Omega$ (see e.g. [4]).

In the non-periodic case, although there still exist an homogenized problem and approximation formula similar to (2), (3), the homogenized matrix A^* is unfortunately unknown a priori. Therefore, one can not replace the numerical resolution of the original problem (1) by that of the homogenized problem (5). Instead, many multiscale numerical methods have been

recently devised in order to solve directly (1) but at a price (in terms of CPU time and memory storage) comparable to that of solving (5). Typically, a multiscale finite element method uses a coarse mesh of size $h > \varepsilon$ and an adapted finite element basis which incorporates the small scale features of the oscillating tensor A^ε. The finite element basis is pre-computed locally on each cell of the coarse mesh (and in parallel for computational efficiency) by solving a local version of (1). The number of degrees of freedom is thus not larger than for a classical finite element method on the coarse mesh.

Let us describe the main idea behind our new multiscale finite element method. Although it is designed for non-periodic homogenization problem, for the sake of simplicity we first present it in the context of periodic homogenization. A key idea is to remark that (2) looks like a first order Taylor expansion, namely it implies

$$u^\varepsilon(x) \approx u^*\left(x + \varepsilon\chi\left(\frac{x}{\varepsilon}\right)\right) \tag{6}$$

where $\chi = (\chi_1, \ldots, \chi_n)$. Building on (6), we introduce a coarse mesh of size $h > \varepsilon$ and a classical conforming finite element basis $\left(\Phi_l^h\right)_l$, and we define an *oscillating finite element basis* through the same composition rule

$$\Phi_l^{\varepsilon,h}(x) = \Phi_l^h\left(x + \varepsilon\chi\left(\frac{x}{\varepsilon}\right)\right).$$

Our method amounts to apply a standard Galerkin procedure to the variational formulation of (1) with this oscillating finite element basis. The advantages of our method are at least twofold. First, it is very easy to implement high order methods since the computation of the oscillating functions $\chi\left(\frac{x}{\varepsilon}\right)$ is independent of the order of the coarse mesh finite element basis $\left(\Phi_l^h\right)_l$. Second, the convergence analysis is somehow simpler since, roughly speaking, it amounts to apply the change of variables $x \to x + \varepsilon\chi\left(\frac{x}{\varepsilon}\right)$ to standard convergence result on the coarse mesh

The content of the paper is as follows. In section 2, we recall some basic facts of homogenization theory and we give a precise statement about (6) in the general (non-periodic) case. Section 3 is devoted to a precise definition of our multiscale finite element method. Its convergence is then studied in section 4. Finally, in section 5 some numerical results are given.

2 Some results in homogenization theory

2.1 H-convergence and oscillating test functions

Let us recall some results of the H-convergence theory (for details see e.g. [15], [2]). Let $\mathcal{M}_n$ be the linear space of square real matrices of order n and define, for given positive constants $\alpha > 0$ and $\beta > 0$, the subspace of $\mathcal{M}_n$ made of matrices which are coercive as well as their inverses

$$\mathcal{M}_{\alpha,\beta} = \left\{M \in \mathcal{M}_n\,;\, M\xi.\xi \geq \alpha|\xi|^2\,,\, M^{-1}\xi.\xi \geq \beta|\xi|^2\,,\, \forall \xi \in \mathbb{R}^n\right\}.$$

A sequence of matrices $A^\varepsilon \in L^\infty(\Omega; \mathcal{M}_{\alpha,\beta})$ is said to H-converge, when ε goes to zero, to a homogenized matrix $A^* \in L^\infty(\Omega; \mathcal{M}_{\alpha,\beta})$ if, for any right hand side $f \in H^{-1}(\Omega)$, the sequence of solutions u^ε of (1) satisfies

$$\begin{aligned} u^\varepsilon &\rightharpoonup u^* \text{ weakly in } H_0^1(\Omega) \quad (\varepsilon \to 0), \\ A^\varepsilon \mathrm{grad}\, u^\varepsilon &\rightharpoonup A^* \mathrm{grad}\, u^* \text{ weakly in } L^2(\Omega)^n \quad (\varepsilon \to 0), \end{aligned}$$

where u^* denotes the solution of the homogenized equation (5). This definition makes sense because of the following sequential compactness property [15].

THEOREM 2.1 *Let $(A^\varepsilon)_{\varepsilon>0}$ be a sequence of matrices in $L^\infty(\Omega;\mathcal{M}_{\alpha,\beta})$. There exists a subsequence, still denoted by ε, and a homogenized matrix $A^* \in L^\infty(\Omega;\mathcal{M}_{\alpha,\beta})$ such that A^ε H-converges to A^*.*

Except in periodic case, this abstract result does not give an explicit formula for the limit A^*. Actually, the homogenized tensor A^* is defined as a limit in the distributional sense, namely

$$A^\varepsilon(x)\,\mathrm{grad}\,\widehat{w}_i^\varepsilon \;\rightharpoonup\; A^* e_i \text{ in } \mathscr{D}'(\Omega;\mathbb{R}^n)$$

where $(e_i)_{i=1,n}$ denotes the canonical basis of $\mathbb{R}^n$, and $(\widehat{w}_i^\varepsilon)_{i=1,n}$ are the so-called *oscillating test functions* which satisfy

$$\widehat{w}_i^\varepsilon \;\rightharpoonup\; x_i \text{ weakly in } H^1(\Omega) \quad (\varepsilon \to 0), \tag{7}$$

and

$$g_i^\varepsilon \;=\; -\mathrm{div}\{A^\varepsilon \mathrm{grad}\,\widehat{w}_i^\varepsilon\} \;\longrightarrow\; g_i \;=\; -\mathrm{div}\{A^* e_i\} \text{ strongly in } H^{-1}(\Omega) \quad (\varepsilon \to 0). \tag{8}$$

The existence of such oscillating test functions is the key point in the proof of Theorem 2.1 but they are neither explicit (they depend on A^*) nor unique (they are unique up to the addition of a sequence converging strongly to zero in $H^1(\Omega)$). For our purpose, we define them as the solutions of the following boundary value problems ($j = 1, ..., n$)

$$\left\{ \begin{array}{rcll} -\mathrm{div}\{A^\varepsilon\,\mathrm{grad}\,\widehat{w}_j^\varepsilon\} & = & -\mathrm{div}\{A^*\,e_j\} & \text{in } \Omega \\ \\ \widehat{w}_j^\varepsilon & = & x_j & \text{on } \partial\Omega. \end{array} \right. \tag{9}$$

These oscillating test functions are also useful for obtaining a corrector result.

THEOREM 2.2 *Let $(A^\varepsilon)_{\varepsilon>0}$ be a sequence H-converging to A^* in $L^\infty(\Omega;\mathcal{M}_{\alpha,\beta})$. Then,*

$$\mathrm{grad}\,u^\varepsilon \;=\; \sum_{i=1}^n \nabla\widehat{w}_i^\varepsilon \frac{\partial u^*}{\partial x_i} \;+\; r_\varepsilon, \tag{10}$$

where the remainder r_ε converges strongly to zero in $L^1(\Omega;\mathbb{R}^n)$. Furthermore, if $u^* \in W^{1,\infty}(\Omega)$, then r_ε converges strongly in $L^2(\Omega;\mathbb{R}^n)$.

REMARK 2.3 *In the context of Theorem 2.2 it is clear that, if the homogenized solution is smoother, say $u \in W^{2,\infty}(\Omega)$, then*

$$u^\varepsilon = u^* + \sum_{i=1}^n (\widehat{w}_i^\varepsilon(x) - x_i)\,\frac{\partial u^*}{\partial x_i} \;+\; r'_\varepsilon \tag{11}$$

where the remainder r'_ε converges strongly to zero in $H^1(\Omega)$. In the sequel, we denote by

$$[\widehat{W}^\varepsilon] \;=\; \left[\left(\frac{\partial\widehat{w}_j^\varepsilon}{\partial x_i}\right]\right)_{i,j=1,n} \tag{12}$$

the so-called corrector matrix.

PROOF: The proof of (10) is classical (see e.g. [2]). The last statement of Theorem 2.2 is simpler to prove, so we briefly explain how to proceed. Using the coercivity of A^ε we are done if we can show that

$$\lim_{\varepsilon\to 0}\int_\Omega A^\varepsilon\left(\text{grad}\,u^\varepsilon\ -\ [\widehat{W}^\varepsilon]\text{grad}\,u^*\right)\cdot\left(\text{grad}\,u^\varepsilon\ -\ [\widehat{W}^\varepsilon]\text{grad}\,u^*\right)\,dx\ =\ 0. \tag{13}$$

Developing the scalar product in the integral (13), we obtain the following terms

$$\int_\Omega [\widehat{W}^\varepsilon]^t A^\varepsilon [\widehat{W}^\varepsilon]\,\text{grad}\,u^*\cdot\text{grad}\,u^*\,dx\ \ +\ \ \int_\Omega A^\varepsilon\,\text{grad}\,u^\varepsilon\cdot\text{grad}\,u^\varepsilon\,dx$$

$$-\ \int_\Omega A^\varepsilon\,\text{grad}\,u^\varepsilon\cdot[\widehat{W}^\varepsilon]\,\text{grad}\,u^*\,dx\qquad -\ \int_\Omega A^\varepsilon\,[\widehat{W}^\varepsilon]\,\text{grad}\,u^*\cdot\text{grad}\,u^\varepsilon\,dx.$$

To pass to the limit in the first term we use the facts (see Lemma 1.3.38 [2]) that $[\widehat{W}^\varepsilon]^t A^\varepsilon[\widehat{W}^\varepsilon]$ converges to A^* in $\mathscr{D}'(\Omega;\mathscr{M}_n)$, and that, thanks to Meyers theorem which implies a uniform $L^p(\Omega)$ bound (with $p>2$) for $[\widehat{W}^\varepsilon]$, this convergence holds true weakly in $L^1(\Omega;\mathscr{M}_n)$. Thus, since $u^*\in W^{1,\infty}(\Omega)$, we have

$$\int_\Omega [\widehat{W}^\varepsilon]^t A^\varepsilon[\widehat{W}^\varepsilon]\,\text{grad}\,u^*\cdot\text{grad}\,u^*\,dx\ \longrightarrow\ \int_\Omega\ A^*\text{grad}\,u^*\cdot\text{grad}\,u^*\,dx.$$

The second term is easy

$$\int_\Omega A^\varepsilon\,\text{grad}\,u^\varepsilon\cdot\text{grad}\,u^\varepsilon\,dx\ =\ \int_\Omega f\,u^\varepsilon\,dx\ \longrightarrow\ \int_\Omega f\,u^*\,dx\ =\ \int_\Omega\ A^*\text{grad}\,u^*\cdot\text{grad}\,u^*\,dx.$$

Applying the "div-curl" compensated compactness result [15] to the third term and using the regularity assumptions as well as Meyers theorem, we get the desired result

$$\int_\Omega A^\varepsilon\,\text{grad}\,u^\varepsilon\cdot[\widehat{W}^\varepsilon]\,\text{grad}\,u^*\,dx\ \longrightarrow\ \int_\Omega\ A^*\text{grad}\,u^*\cdot\text{grad}\,u^*\,dx.$$

The fourth term is treated in the same way and their combination gives zero. ∎

2.2 A remark on the corrector result

The right hand side of formula (11) looks like the first order Taylor expansion of u^* at the point $\widehat{w}^\varepsilon(x)=(\widehat{w}_1^\varepsilon(x),...,\widehat{w}_n^\varepsilon(x))$. It indicates that $u^\varepsilon(x)$ may well be approximated by $u^*\circ\widehat{w}^\varepsilon(x)$. This remark is at the basis of the new form of the corrector result (Theorem 2.2) that we now propose.

THEOREM 2.4 *Let $(A^\varepsilon)_{\varepsilon>0}$ be a sequence H-converging to A^* in $L^\infty(\Omega;\mathcal{M}_{\alpha,\beta})$. For $f\in H^{-1}(\Omega)$, let u^ε be the solution of (1) and u^* be that of (5). Let $\widehat{w}_j^\varepsilon$ be the family of oscillating test functions defined in (9). Assume that $u^*\in W^{2,\infty}(\Omega)$ and $\widehat{w}^\varepsilon$ is uniformly bounded in $L^q(\Omega)^n$ for any $2\le q<+\infty$. Then*

$$u^\varepsilon\ =\ u^*\circ\widehat{w}^\varepsilon\ +\ \widehat{r}^\varepsilon, \tag{14}$$

where the remainder term $\widehat{r}^\varepsilon$ converges strongly to zero in $H_0^1(\Omega)$.

REMARK 2.5 *In space dimension $n=2$, since $H^1(\Omega)\subset L^q(\Omega)$ for any $2\le q<+\infty$, there is no additional assumption on $\widehat{w}^\varepsilon$ in Theorem 2.4. If $\widehat{w}^\varepsilon$ is not uniformly bounded in any $L^q(\Omega)^n$, it is at least bounded in $L^{2^*}(\Omega)^n$ with $2^*=2n/(n-2)$ and we can still obtain the strong convergence to zero of $\widehat{r}^\varepsilon$ in $W^{1,n/(n-1)}(\Omega)$.*

REMARK 2.6 *The approximation of* the principal part of the solution u^ε, *i.e.* $u^*\circ\widehat{w}^\varepsilon$, *may serve as a substitute for the approximation of the solution of problem (1). This idea is at the root of the new multiscale finite element method described in this work.*

PROOF: It is not clear that $\widehat{w}^\varepsilon(\Omega) \subset \Omega$ (see remark 2.10), so formula (14) makes sense if u^* is first extended by zero outside Ω. Since u^* is a Lipschitz function, $u^* \circ \widehat{w}^\varepsilon$ belongs to $H^1(\Omega)$. Furthermore, since $\widehat{w}^\varepsilon(x) = x$ a.e. on $\partial\Omega$, the function $u^* \circ \widehat{w}^\varepsilon$ belongs to $H_0^1(\Omega)$. We have

$$\|u^\varepsilon \ - \ u^* \circ \widehat{w}^\varepsilon\|_{H_0^1(\Omega)} \ = \ \|\mathrm{grad}\, u^\varepsilon \ - \ \mathrm{grad}\,(\, u^* \circ \widehat{w}^\varepsilon)\|_{L^2(\Omega)^n}$$

$$\leq \ \|\mathrm{grad}\, u^\varepsilon \ - \ [\widehat{W}^\varepsilon]\, \mathrm{grad}\, u^*\|_{L^2(\Omega)^n} \ + \ \|[\widehat{W}^\varepsilon]\ (\ \mathrm{grad}\, u^* \ - \ (\mathrm{grad}\, u^*) \circ \widehat{w}^\varepsilon)\ \|_{L^2(\Omega)^n}. \qquad (15)$$

The first term in the right hand side of (15) goes to zero because of Theorem 2.2. The second term is bounded by

$$\|[\widehat{W}^\varepsilon]\ (\ \mathrm{grad}\, u \ - \ (\mathrm{grad}\, u) \circ \widehat{w}^\varepsilon)\ \|_{L^2(\Omega)^n} \ \leq \ \|[\widehat{W}^\varepsilon]\|_{L^p(\Omega;\mathcal{M}_n)} \ \|\mathrm{grad}\, u^* \ - \ (\mathrm{grad}\, u^*) \circ \widehat{w}^\varepsilon\|_{L^{p'}(\Omega)^n}$$

with $1/p + 1/p' = 1/2$. A Taylor expansion with integral rest yields

$$(\mathrm{grad}\, u^*) \circ \widehat{w}^\varepsilon \ = \ \mathrm{grad}\, u^* \ + \ \int_0^1 \ \nabla\nabla\, u^*(x + t(\widehat{w}^\varepsilon(x) - x)).(\widehat{w}^\varepsilon(x) - x)\, dt$$

and thus, we obtain

$$\|(\mathrm{grad}\, u^*) \circ \widehat{w}^\varepsilon \ - \ \mathrm{grad}\, u^*\|_{L^{p'}(\Omega)^n} \ \leq \ \|u^*\|_{W^{2,\infty}(\Omega)}\| \ \widehat{w}^\varepsilon - x\|_{L^{p'}(\Omega;\mathbb{R}^n)^n}.$$

By Meyers theorem there exists $p > 2$ such that $\|[\widehat{W}^\varepsilon]\|_{L^p(\Omega;\mathcal{M}_n)}$ is uniformly bounded. By assumption $(\widehat{w}^\varepsilon - x)$ is bounded in any $L^q(\Omega;\mathbb{R}^n)^n$, $2 \leq q < +\infty$, and since it converges strongly to zero in $L^2(\Omega;\mathbb{R}^n)^n$, it also converges strongly in $L^{p'}(\Omega;\mathbb{R}^n)^n$. All together this implies that the second term in the right hand side of (15) goes to zero. ∎

There is a converse statement of Theorem 2.4.

THEOREM 2.7 *Let $(A^\varepsilon)_{\varepsilon>0}$ be a sequence H-converging to A^* in $L^\infty(\Omega;\mathcal{M}_{\alpha,\beta})$. For $f \in H^{-1}(\Omega)$, let u^ε be the solution of (1) and $\widehat{w}^\varepsilon$ be the family of oscillating test functions defined in (9). If there exists a function $u \in H_0^1(\Omega) \cap W^{1,\infty}(\Omega)$ such that*

$$\|u^\varepsilon \ - \ u \circ \widehat{w}^\varepsilon\|_{H_0^1(\Omega)} \ \longrightarrow \ 0 \ \textit{when} \ \varepsilon \to 0,$$

then $u = u^*$, the solution of the homogenized problem (5).

PROOF: By assumption, u^ε admits the following representation formula, similar to (14),

$$u^\varepsilon \ = \ u \circ \widehat{w}^\varepsilon \ + \ \tilde{r}^\varepsilon, \qquad (16)$$

where $\tilde{r}^\varepsilon$ converges strongly to zero in $H_0^1(\Omega)$. Let us consider the variational formulation of (1)

$$a^\varepsilon(u^\varepsilon, v) \ = \ \int_\Omega A^\varepsilon \mathrm{grad}\, u^\varepsilon \cdot \mathrm{grad}\, v\, dx \ = \ \int_\Omega f\ v\, dx \ , \ \forall v \in H_0^1(\Omega). \qquad (17)$$

Substituting (16) into (17) gives

$$\int_\Omega A^\varepsilon [\widehat{W}^\varepsilon]\, (\mathrm{grad}\, u) \circ \widehat{w}^\varepsilon \cdot \mathrm{grad}\, v\, dx \ + \ \int_\Omega A^\varepsilon \mathrm{grad}\, \tilde{r}^\varepsilon \cdot \mathrm{grad}\, v\, dx \ = \ \int_\Omega f\ v\, dx\ , \ \forall v \in H_0^1(\Omega).$$

By assumption the second integral goes to zero, while the first one converges to $\int_\Omega A^* \nabla u \cdot \nabla v\, dx$. Indeed, by H-convergence, $A^\varepsilon[\widehat{W}^\varepsilon]$ converges weakly to A^* in $L^2(\Omega;\mathscr{M}_n)$ and, by the Lebesgue dominated convergence theorem, $(\mathrm{grad}\, u) \circ \widehat{w}^\varepsilon$ converges strongly to $\mathrm{grad}\, u$ in $L^2(\Omega)^n$. Thus, passing to the limit we obtain that u is a solution of the variational formulation of the homogenized problem (5), i.e. $u = u^*$. ∎

2.3 An approximate variational formulation

The representation formula (14) for u_ε suggests an approximation of the variational formulation (17). Indeed, it is equivalent to

$$a^\varepsilon(\, u^* \circ \widehat{w}^\varepsilon \,,\, v \,) \;=\; \int_\Omega f\, v\, dx \;-\; a^\varepsilon(\, \widehat{r}^\varepsilon \,,\, v \,) \;,\; \forall v \in H_0^1(\Omega), \tag{18}$$

where the last term goes to zero. Dropping it and choosing an adequate subspace of $H_0^1(\Omega)$ should yield a good approximation of (17). A first possible choice of subspace is

$$\left\{ v^\varepsilon \in H_0^1(\Omega) \,;\, \exists\, v \in H_0^1(\Omega) \cap W^{1,\infty}(\Omega) \,,\, v^\varepsilon \;=\; v \circ \widehat{w}^\varepsilon \right\},$$

but it is unfortunately not closed in $H_0^1(\Omega)$, so it can not be a Hilbert space. Another possibility, which requires the additional regularity $\widehat{w}^\varepsilon \in W^{1,\infty}(\Omega;\mathbb{R}^n)$, is

$$V^\varepsilon \;=\; \left\{ v^\varepsilon \in H_0^1(\Omega) \,;\, \exists\, v \in H_0^1(\Omega) \,,\, v^\varepsilon \;=\; v \circ \widehat{w}^\varepsilon \right\}, \tag{19}$$

which is a closed subspace of $H_0^1(\Omega)$ since $\widehat{w}^\varepsilon \in W^{1,\infty}(\Omega;\mathbb{R}^n)$ implies that $v \circ \widehat{w}^\varepsilon$ belongs to $H_0^1(\Omega)$ as soon as v does. We defined the approximate variational formulation as: find $u \in H_0^1(\Omega)$ such that

$$a^\varepsilon(u \circ \widehat{w}^\varepsilon, v \circ \widehat{w}^\varepsilon) \;=\; \int_\Omega f v \circ \widehat{w}^\varepsilon dx \;,\; \forall v \in H_0^1(\Omega). \tag{20}$$

By the Lax-Milgram theorem (20) admits a unique solution $u \circ \widehat{w}^\varepsilon$ in V^ε. In the following, we will call *u the substituting homogenized solution*. Remark that, u actually depends on ε but it oscillates less compared to u_ε.

LEMMA 2.8 *Assume $\widehat{w}^\varepsilon \in W^{1,\infty}(\Omega;\mathbb{R}^n)$. Let u be the unique solution of (20) and u^* be the solution of the homogenized problem (5). Then*

$$\|(u - u^*) \circ \widehat{w}^\varepsilon\|_{H_0^1(\Omega)} \;\to\; 0 \quad \textit{when } \varepsilon \to 0.$$

REMARK 2.9 *Of course, combining Lemma 2.8 and our corrector result Theorem 2.4, we deduce that $u \circ \widehat{w}^\varepsilon$ is a good approximation of the solution u_ε of the original problem (1)*

$$\|u^\varepsilon - u \circ \widehat{w}^\varepsilon\|_{H_0^1(\Omega)} \;\to\; 0 \quad \textit{when } \varepsilon \to 0.$$

PROOF: Subtracting (20) from (18) with the same test function $(v \circ \widehat{w}^\varepsilon) \in V^\varepsilon \subset H_0^1(\Omega)$ we obtain

$$a^\varepsilon(\, (u - u^*) \circ \widehat{w}^\varepsilon \,,\, v \circ \widehat{w}^\varepsilon \,) \;=\; a^\varepsilon(\, \widehat{r}^\varepsilon \,,\, v \circ \widehat{w}^\varepsilon \,).$$

Taking $v = u - u^*$, using coercivity and continuity of the bilinear form show that

$$\alpha\, \|(u - u^*) \circ \widehat{w}^\varepsilon\|_{H_0^1(\Omega)} \;\le\; \beta^{-1}\; \|\widehat{r}^\varepsilon\|_{H_0^1(\Omega)},$$

which goes to zero as ε does. ∎

2.4 Change of variables

A reasonable question to ask is whether the mapping $x \to w^\varepsilon(x)$ from Ω into $\mathbb{R}^n$ is a change of variables, i.e. is one-to-one into Ω. We do not know if it is true in general. Nevertheless we have the following partial results.

LEMMA 2.10 *Assume $\widehat{w}^\varepsilon \in W^{1,\infty}(\Omega)^n$. Then, the mapping $\widehat{w}^\varepsilon$ is onto in the sense that $\widehat{w}^\varepsilon(\overline{\Omega}) \supset \overline{\Omega}$.*

PROOF: Since $\widehat{w}^\varepsilon = x \,\text{on}\, \partial\Omega$ and $W^{1,\infty}(\Omega) \subset C^0(\overline{\Omega})$ then, from topological degree theory [16],

$$deg(\widehat{w}^\varepsilon, \Omega, y) = deg(id, \Omega, y) \ \forall y \notin \partial\Omega$$

where id denotes the canonical injection from Ω into $\mathbb{R}^n$. On the other hand,

$$deg(id, \Omega, y) = \begin{cases} 1 \,\text{if}\, y \in \Omega \\ \\ 0 \,\text{if}\, y \notin \Omega. \end{cases}$$

thus, for $y \in \Omega$, $deg(\widehat{w}^\varepsilon, \Omega, y) \neq 0$ and from topological degree property, we deduce that there exists an $x \in \Omega$ such that $y = \widehat{w}^\varepsilon(x)$. ∎

The question of injectivity is much more delicate. Let us simply recall the following result of [1].

THEOREM 2.11 *Assume $\Omega \subset \mathbb{R}^2$ is a bounded simply connected open set, whose boundary $\partial\Omega$ is a convex closed curve. Assume further that $A^\varepsilon(x)$ is symmetric and that A^* does not depend on x. Then, the mapping $\widehat{w}^\varepsilon$ is a homeomorphism from $\overline{\Omega}$ into itself.*

REMARK 2.12 *The homogenized matrix A^* is constant, for example, in the case of periodic homogenization, i.e. $A^\varepsilon(x) = A(\frac{x}{\varepsilon})$.*

REMARK 2.13 *In the case of small amplitude homogenization, one can prove that the mapping $\widehat{w}^\varepsilon$ is a homeomorphism. Indeed, by a perturbation argument, if $A^\varepsilon(x)$ is close to a constant matrix A_0, then $\widehat{w}^\varepsilon(x)$ is close to x and thus is one-to-one.*

3 Definition of the multiscale finite element method

3.1 Approximation of the oscillating test functions

The idea of our multiscale finite element method is to solve the approximate variational formulation (20) instead of the true one (17). This requires the computation of the oscillating test functions which are not explicit since, in view of their definition (9), they depend on A^* which is unknown. Therefore, we need to introduce an adequate approximation procedure.
We introduce a coarse mesh of Ω which, for simplicity, is assumed to be polyhedral. This coarse mesh is a conformal triangulation $\mathcal{T}_h$ such that

$$\overline{\Omega} = \bigcup_{K \in \mathcal{T}_h} K \tag{21}$$

where the elements K satisfy $\text{diam}(K) \leq h$. In practice the mesh size h is larger than the space scale of oscillations ε, i.e. $h > \varepsilon$. For each $K \in \mathcal{T}_h$, let us define $\widehat{w}_i^{\varepsilon,K}$ $(i = 1, ..., n)$ as the solution of

$$\begin{cases} -\text{div}\{A^\varepsilon \,\text{grad}\, \widehat{w}_i^{\varepsilon,K}\} = -\text{div}\{A_K^* \,\text{grad}\, x_i\} & \text{in } K, \\ \\ \widehat{w}_i^{\varepsilon,K} = x_i & \text{on } \partial K, \end{cases} \tag{22}$$

where A_K^* is a local approximation of A^* in K. The simplest approximation is to take A_K^* constant in K : in such a case its precise value is irrelevant since the right hand side of (22) cancels out. This will be our choice in the numerical examples of this paper. Nevertheless, it is possible to take $A_K^*(x)$ as some varying local average of A^ε.

Collecting together these local approximations we define $\widehat{w}_i^{\varepsilon,h} \in H^1(\Omega)$ by $\widehat{w}_i^{\varepsilon,h} = \widehat{w}_i^{\varepsilon,K}$ for each $K \in \mathcal{T}_h$, and we set $\widehat{w}^{\varepsilon,h} = \left(\widehat{w}_1^{\varepsilon,h}, \ldots, \widehat{w}_n^{\varepsilon,h}\right) \in H^1(\Omega; \mathbb{R}^n)$.

A numerical approximation of the local oscillating test functions defined in (22) is computed by using a classical conforming finite element in each $K \in \mathcal{T}_h$. For each coarse mesh cell K we introduce a local fine mesh $\mathcal{T}_{h'}^K$ where h' denotes the size of this fine mesh. Of course, we have $h' < h$, but, since we want to resolve the oscillations of the tensor A^ε, we also have $h' < \varepsilon$. Typically we use $\mathbb{P}_{k'}$ Lagrange finite elements for solving the local boundary value problems (22). Since, from one cell K to the other, these problems are independent this may be done in parallel. This procedure is very similar to that introduced in [11].

The *hats* used in our notation refer to exact solutions of boundary value problems : thus, $\widehat{w}^\varepsilon$ refers to the "true" oscillating test function and $\widehat{w}^{\varepsilon,h}$ refers to the collection over $\mathcal{T}_h$ of all solutions of (22). We shall drop the *hat notation* when we refer to the corresponding numerical approximations: thus $w_i^{\varepsilon,K}$ is the $\mathbb{P}_{k'}$ finite element approximation of $\widehat{w}_i^{\varepsilon,K}$, and $w_i^{\varepsilon,h}$, $w^{\varepsilon,h}$ are defined as above with the hat notation.

REMARK 3.1 *The domain of definition of the local oscillating test functions $\widehat{w}_i^{\varepsilon,K}$ is exactly the cell K. However, one can possibly define it on a larger domain (even if only its restriction to K is used). For instance, in order to prevent boundary layer effects we can devise a so-called oversampling method in the spirit of [11] by solving (22) in a domain Q which is slightly larger than K. In the context of [11] this yields to a non-conforming finite element method which is analyzed in [9]. In our framework, the oversampling method is still a conforming finite element method (see Remark 3.4).*

REMARK 3.2 *In many applications, like composite materials, the coefficient matrix A^ε is discontinuous and thus the oscillating test function $\widehat{w}^{\varepsilon,h}$ does not have a second derivative. In such a case, as is well known, using higher order finite elements does not improve the convergence rate, so we content ourselves in using $\mathbb{P}_1$ finite elements for computing $w^{\varepsilon,h}$.*

3.2 A multiscale finite element method

Let $V_h \subset H_0^1(\Omega)$ be a finite dimensional subspace ($\dim V_h = N_h$) corresponding to a conforming finite element method defined on the coarse mesh (22). Typically we use $\mathbb{P}_k$ Lagrange finite elements. Let $\left(\Phi_l^h\right)_{l=1,...,N_h}$ denote a finite element basis of V_h. In order to compute a numerical approximation u_h of the substituting homogenized solution u, we introduce an *oscillating (or multiscale) finite element basis* defined by

$$\Phi_l^{\varepsilon,h}(x) \;=\; \Phi_l^h \circ w^{\varepsilon,h}(x)\,,\;\; (l = 1, ..., N_h). \tag{23}$$

We therefore obtain a conformal finite element method associated to the coarse mesh $\mathcal{T}_h$ and we denote by $V_h^\varepsilon \subset H_0^1(\Omega)$ the space spanned by the functions $\left(\Phi_l^{\varepsilon,h}\right)_{l=1,...,N_h}$. Roughly speaking, V_h^ε is the space "$V_h \circ w^{\varepsilon,h}$".

¿From the approximate variational formulation (20), we deduce a numerical approximation: find $u_h \circ w^{\varepsilon,h} \in V_h^\varepsilon$ such that

$$a^\varepsilon(u_h \circ w^{\varepsilon,h}, v_h \circ w^{\varepsilon,h}) \;=\; \int_\Omega f\; v_h \circ w^{\varepsilon,h}\, dx \;\;,\;\; \forall v_h \circ w^{\varepsilon,h} \in V_h^\varepsilon. \tag{24}$$

We use Lagrange finite elements and consequently the degrees of freedom are the values at the nodes n_j^K ($j = 1, ..., N_K$) of the elements $K \in \mathcal{T}_h$. For such an element K, let $\Phi^{\varepsilon,K}$ be the associated local basis which is made of N_K polynomials $p_i^K \in \mathbb{P}_k$ satisfying $p_i^K(n_j^K) = \delta_{ij}$. The local oscillating finite element basis is

$$\Phi_i^{\varepsilon,K}(x) \;=\; p_i^K \circ w^{\varepsilon,K}(x) \tag{25}$$

and, since $w^{\varepsilon,K}(x) = x$ on ∂K, it still satisfies

$$\Phi_i^{\varepsilon,K}(n_j^K) \;=\; \delta_{ij}.$$

On the other hand, for each $K \in \mathcal{T}_h$,

$$(u_h \circ w^{\varepsilon,K})|_K(x) \;=\; [\Phi^{\varepsilon,K}(x)]\,\{u_h^K\}$$

where $[\Phi^{\varepsilon,K}(x)] = [\Phi_1^{\varepsilon,K}, ..., \Phi_{N_K}^{\varepsilon,K}]$ and $\{u_h^K\}$ is the column vector composed of values of u_h at the nodes of K.

REMARK 3.3 *In the case of piecewise linear finite elements $\mathbb{P}_1$ we recover the multiscale finite element method previously introduced by T. Hou and X.-H. Wu [11]. Indeed, when the basis functions p_i^K belong to $\mathbb{P}_1$, by linearity the oscillating basis functions can be written*

$$\Phi_i^{\varepsilon,K}(x) \;=\; p_i^K(x) \;+\; \sum_{j=1}^{n} \Big(w_j^{\varepsilon,K}(x) - x_j \Big)\, \frac{\partial p_i^K}{\partial x_j}(x). \tag{26}$$

A simple calculus shows that

$$\mathrm{div}\{A^\varepsilon \,\mathrm{grad}\, \Phi_i^{\varepsilon,K}\} \;\;=\;\; \sum_{j=1}^{n} \mathrm{div}\{A^\varepsilon \mathrm{grad}\, w_j^{\varepsilon,K}\} \frac{\partial p_i^K}{\partial x_j} \quad \text{in } K$$

and, if we choose A_K^* constant in the definition (22), we obtain

$$\left\{ \begin{array}{rcll} -\mathrm{div}\{A^\varepsilon \,\mathrm{grad}\, \Phi_i^{\varepsilon,K}\} & = & 0 & \text{in } K \\ \\ \Phi_i^{\varepsilon,K} & = & p_i & \text{on } \partial K \end{array} \right. \tag{27}$$

which is precisely the definition of the finite element basis in the multiscale method of T. Hou and X.-H. Wu [11].

REMARK 3.4 *As explained in Remark 3.1 we can devise an oversampling method in the spirit of [11], [9]. If the local oscillating test functions $w_i^{\varepsilon,K}$ are computed from (22) in a domain Q which is larger than K, the composition with Φ_l^h is still going to define a conforming finite element basis. However, the support of $\Phi_l^{\varepsilon,h}$ may now be different from that of Φ_l^h and its nodal values are also different.*

4 Convergence proof in the periodic case

Although for its practical implementation our multiscale numerical method does not make any assumption on the possible type of heterogeneities or oscillations of the tensor A^ε, it is convenient to analyze its convergence in the context of periodically oscillating coefficients. In this section, we assume that $A^\varepsilon(x) = A(\frac{x}{\varepsilon})$ where $A(y)$ is a periodic, uniformly coercive and bounded, matrix in the unit cube $Y = (0,1)^n$. As is usual practice in the numerical analysis of finite element methods, we assume that the tensor $A(y)$ is smooth in order to use classical result from this field. However, from the point of view of homogenization theory, it is enough to assume that $A(y)$ is piecewise smooth, possibly discontinuous through smooth interfaces, since this implies that the solutions of the cell problem (4) and those of (22) (which defines the oscillating test functions) belong to $W^{1,\infty}$ which is just enough for our analysis.

Recall that we use a $\mathbb{P}_k$ Lagrange finite element method ($k \geq 1$) on the coarse mesh of size h, and, locally on each cell K of the coarse mesh, a $\mathbb{P}_{k'}$ Lagrange finite element method on a fine mesh of size h' to compute the oscillating test functions. We always assume that

$$0 < h' < \varepsilon < h < 1.$$

THEOREM 4.1 *Let u^ε be the exact solution of (1) and $u_h^\varepsilon \equiv u_h \circ w^{\varepsilon,h}$ be the numerical solution of (24). Assume that $u^* \in W^{k+1,\infty}(\Omega)$ and $\chi_i \in W^{1,\infty}(Y)$. There exists a constant C independent of ε and h such that*

$$\|u^\varepsilon - u_h^\varepsilon\|_{H_0^1(\Omega)} \leq C\left(h^k + \sqrt{\frac{\varepsilon}{h}} + \left(\frac{h'}{\varepsilon}\right)^{k'}\right). \tag{28}$$

REMARK 4.2 *Using an oversampling method as explained in Remarks 3.1 and 3.4 would improve slightly estimate (28) by replacing the $\sqrt{\varepsilon/h}$ term in its right hand side (which is due to boundary layer effects) with ε/h. However, the resonance effect (i.e. the fact that method does not converge if $h \approx \varepsilon$) does not disappear.*

PROOF: ¿From Céa's lemma [7] applied to (24), there exists a constant C independent of ε and h such that

$$\|u^\varepsilon - u_h^\varepsilon\|_{H_0^1(\Omega)} \leq C \inf_{v_h^\varepsilon \in V_h^\varepsilon} \|u^\varepsilon - v_h^\varepsilon\|_{H_0^1(\Omega)}. \tag{29}$$

Define Π_h as the V_h-interpolation operator: $\Pi_h\, v(x) = \sum_{l=1}^{N_h} v(n_l)\Phi_l^h(x)$ where n_l denotes the nodes associated to the $\mathbb{P}_k$ finite element method. In the same way Π_h^ε denotes the V_h^ε-interpolation operator: $\Pi_h^\varepsilon\, v(x) = \sum_{l=1}^{N_h} v(n_l)\Phi_l^{\varepsilon,h}(x)$. It satisfies $\Pi_h^\varepsilon\, v = (\Pi_h\, v) \circ w^{\varepsilon,h}$.

In (29) we choose $v_h^\varepsilon = \Pi_h^\varepsilon u^*$ where u^* is the exact solution of the homogenized problem (5). This yields

$$\|u^\varepsilon - u_h^\varepsilon\|_{H_0^1(\Omega)} \leq C\,\|u^\varepsilon - \Pi_h^\varepsilon u^*\|_{H_0^1(\Omega)}. \tag{30}$$

Introducing the rescaled solution of the cell problem (4)

$$\widetilde{w}^\varepsilon(x) = x + \varepsilon\chi\left(\frac{x}{\varepsilon}\right), \tag{31}$$

we bound the right hand side of (30)

$$\begin{aligned}
\|\nabla u^\varepsilon - \nabla(\Pi_h^\varepsilon u^*)\|_{L^2(\Omega)^n} \leq C \Big(& \|\nabla u^\varepsilon - \nabla\,(u^* \circ \widetilde{w}^\varepsilon)\,\|_{L^2(\Omega)^n} \\
& + \|\nabla\{(\,u^* - \Pi_h u^*) \circ \widetilde{w}^\varepsilon\}\|_{L^2(\Omega)^n} \\
& + \|\nabla\{\Pi_h u^* \circ (\,\widetilde{w}^\varepsilon - \widehat{w}^{\varepsilon,h}\,)\}\|_{L^2(\Omega)^n} \\
& + \|\nabla\{\Pi_h u^* \circ (\,\widehat{w}^{\varepsilon,h} - w^{\varepsilon,h}\,)\}\|_{L^2(\Omega)^n} \Big).
\end{aligned} \tag{32}$$

The upper bound (32), which gives the order of convergence of our multiscale finite element method, is made of four terms. The first one is related to a corrector result in periodic homogenization. The second one is linked to an interpolation result for the coarse mesh $\mathbb{P}_k$ finite element method. The third one is related to an homogenization result for the local oscillating test functions. Finally the fourth term is concerned with an error estimate for the $\mathbb{P}_{k'}$ finite element method used to compute the local oscillating test functions.

The first term in the right hand side of (32) is bounded thanks to Lemma 4.4. The second term is

$$\|[\nabla\widetilde{w}^\varepsilon]\{\nabla(\,u^* - \Pi_h u^*)\} \circ \widetilde{w}^\varepsilon\|_{L^2(\Omega)^n} \leq \|Id + [\nabla_y\chi]\|_{L^\infty(Y)}\|\{\nabla(\,u^* - \Pi_h u^*)\} \circ \widetilde{w}^\varepsilon\|_{L^2(\Omega)^n}. \tag{33}$$

To estimate the right hand side of (33) we perform a Taylor expansion with integral rest

$$\{\nabla(\,u^* - \Pi_h u^*)\} \circ \widetilde{w}^\varepsilon = \nabla(\,u^* - \Pi_h u^*)(x) + \varepsilon\int_0^1 \nabla\nabla(\,u^* - \Pi_h u^*\,)\left(x + \varepsilon t\chi(\frac{x}{\varepsilon})\right)\cdot\chi\left(\frac{x}{\varepsilon}\right)\,dt$$

and thus (33) is bounded by

$$\|Id + [\nabla_y \chi]\|_{L^\infty(Y)} \left(\|u^* - \Pi_h u^*\|_{H^1(\Omega)} + \varepsilon \|u^* - \Pi_h u^*\|_{W^{2,\infty}(\Omega)} \|\chi\|_{L^2(Y)} \right)$$
$$\leq \|Id + [\nabla_y \chi]\|_{L^\infty(Y)} \|u^*\|_{W^{k+1,\infty}(\Omega)} \left(h^k + \varepsilon h^{k-1} \|\chi\|_{L^2(Y)} \right)$$

by standard interpolation results for Lagrange $\mathbb{P}_k$ finite elements [7]. Remark that the above Taylor expansion is valid only if the interpolate $\Pi_h u^*$ admits a second derivative, which is true if the finite element order is $k \geq 2$. For $k = 1$ the argument must be slightly changed, but, since in such a case our method coincides with that in [11], [12], we do not give unnecessary details.

The third term in the right hand side of (32) is

$$\|[\nabla(\widetilde{w}^\varepsilon - \widehat{w}^{\varepsilon,h})]\{\nabla(\Pi_h u^*)\} \circ (\widetilde{w}^\varepsilon - \widehat{w}^{\varepsilon,h})\|_{L^2(\Omega)^n} \leq \|u^*\|_{W^{1,\infty}(\Omega)} \|\nabla(\widetilde{w}^\varepsilon - \widehat{w}^{\varepsilon,h})\|_{L^2(\Omega)^n}. \quad (34)$$

To estimate the right hand side of (34) we write

$$\|\nabla(\widetilde{w}^\varepsilon - \widehat{w}^{\varepsilon,h})\|^2_{L^2(\Omega)^n} = \sum_{K \in \mathcal{T}_h} \|\nabla(\widetilde{w}^\varepsilon - \widehat{w}^{\varepsilon,h})\|^2_{L^2(K)^n}$$

and we use Lemma 4.3 for each cell K: actually, $\widehat{w}^{\varepsilon,h}$ converges to x in $H^1(K)$ weakly as ε goes to 0 (for fixed h), so $\widetilde{w}^\varepsilon$ is exactly the sum of the homogenized limit and of the corrector term. Since K is of size h, its surface $|\partial K|$ is of order h^{n-1} and the total number of cells K is of order h^{-n}. Thus, we obtain

$$\|\nabla(\widetilde{w}^\varepsilon - \widehat{w}^{\varepsilon,h})\|^2_{L^2(\Omega)^n} \leq C \frac{\varepsilon}{h}.$$

Finally the fourth term in the right hand side of (32) is

$$\|[\nabla(\widehat{w}^{\varepsilon,h} - w^{\varepsilon,h})]\{\nabla(\Pi_h u^*)\} \circ (\widehat{w}^{\varepsilon,h} - w^{\varepsilon,h})\|_{L^2(\Omega)^n} \leq \|u^*\|_{W^{1,\infty}(\Omega)} \|\nabla(\widehat{w}^{\varepsilon,h} - w^{\varepsilon,h})\|_{L^2(\Omega)^n}. \quad (35)$$

In the right hand side of (35) we have the difference between an exact cell solution $\widehat{w}^{\varepsilon,h}$ and its numerical approximation $w^{\varepsilon,h}$. By standard interpolation results for Lagrange $\mathbb{P}_{k'}$ finite elements [7] (valid if the tensor $A(y)$ is smooth enough), we thus obtain

$$\|\nabla(\widehat{w}^{\varepsilon,h} - w^{\varepsilon,h})\|^2_{L^2(\Omega)^n} = \sum_{K \in \mathcal{T}_h} \|\nabla(\widehat{w}^{\varepsilon,h} - w^{\varepsilon,h})\|^2_{L^2(K)^n} \leq C(h')^{2k'} \sum_{K \in \mathcal{T}_h} |\widehat{w}^{\varepsilon,h}|^2_{H^{k'+1}(K)}.$$

Then, assuming again that $A(y)$ is smooth enough, the oscillating test function is also smooth and satisfies

$$|\widehat{w}^{\varepsilon,h}|_{H^{k'+1}(K)} \leq C \varepsilon^{-k'} \sqrt{|K|}.$$

Collecting together all four terms, (32) yields

$$\|\nabla u^\varepsilon - \nabla(\Pi_h^\varepsilon u^*)\|_{L^2(\Omega)^n} \leq C \left(\sqrt{\varepsilon} + (h^k + \varepsilon h^{k-1}) + \sqrt{\frac{\varepsilon}{h}} + \left(\frac{h'}{\varepsilon} \right)^{k'} \right),$$

which implies (28). ∎

We now recall a classical corrector result in periodic homogenization [5] where the dependence on the size of the domain is made explicit (for a proof, see [11]). Let ω be a smooth bounded open set, $f \in L^2(\omega)$ and $g \in H^1(\omega)$. Define the original problem

$$\left\{ \begin{array}{rcll} -\mathrm{div}\{A^\varepsilon \, \mathrm{grad}\, v^\varepsilon\} & = & f & \text{in } \omega, \\ v^\varepsilon & = & g & \text{on } \partial\omega, \end{array} \right.$$

and its homogenized limit

$$\left\{ \begin{array}{rcll} -\mathrm{div}\{A^* \, \mathrm{grad}\, v^*\} & = & f & \text{in } \omega, \\ v^* & = & g & \text{on } \partial\omega. \end{array} \right.$$

LEMMA 4.3 *There exists a constant C, which is independent of ε, ω and the data f, g, such that*

$$\left\| v^\varepsilon \ - \ v^* \ - \ \varepsilon \sum_{i=1}^{n} \chi_i \left(\frac{x}{\varepsilon} \right) \frac{\partial v^*}{\partial x_i}(x) \right\|_{H^1(\omega)} \ \leq \ C\sqrt{\varepsilon} \ \sqrt{|\partial\omega|} \ \|v^*\|_{W^{2,\infty}(\omega)}.$$

The next lemma is a quantitative version of Theorem 2.4 in the periodic case. Remark however that it involves the solution of the cell problem instead of the oscillating test function $\widehat{w}^\varepsilon$ defined by (9).

LEMMA 4.4 *Let $\widetilde{w}^\varepsilon$ be defined by (31). Assume that $u^* \in W^{2,\infty}(\Omega)$ and $\chi_i \in W^{1,\infty}(Y)$. Then, there exists a constant C, independent of ε, such that*

$$\|u^\varepsilon \ - \ u^* \circ \widetilde{w}^\varepsilon\|_{H_0^1(\Omega)} \ \leq \ C\sqrt{\varepsilon}.$$

PROOF: We have

$$\begin{array}{rcl} \|\nabla \, u^\varepsilon \ - \ \nabla \, (\, u^* \circ \widetilde{w}^\varepsilon)\|_{L^2(\Omega)^n} & \leq & \|\nabla \, u^\varepsilon \ - \ [\nabla \widetilde{w}^\varepsilon] \, \nabla \, u^*\|_{L^2(\Omega)^n} \\ & + & \|[\nabla \widetilde{w}^\varepsilon] \ (\, \nabla \, u^* \ - \ (\nabla \, u^*) \circ \widetilde{w}^\varepsilon) \, \|_{L^2(\Omega)^n}. \end{array} \tag{36}$$

Since $[\nabla \widetilde{w}^\varepsilon(x)] = Id + [\nabla_y \chi] \, (\frac{x}{\varepsilon})$, the first term in the right hand side of (36) is bounded by $\sqrt{\varepsilon}$ by a classical corrector result (see Lemma 4.3). The second term is bounded by

$$\|Id + [\nabla_y \chi]\|_{L^\infty(Y)} \ \|\nabla \, u^* \ - \ (\nabla \, u^*) \circ \widetilde{w}^\varepsilon\|_{L^2(\Omega)^n}.$$

A Taylor expansion with integral rest yields

$$(\nabla \, u^*) \circ \widetilde{w}^\varepsilon \ = \ \nabla \, u^* \ + \ \varepsilon \int_0^1 \ \nabla\nabla \, u^* \left(x + \varepsilon t \chi(\frac{x}{\varepsilon}) \right) \cdot \chi \left(\frac{x}{\varepsilon} \right) \, dt$$

and thus, we obtain

$$\|(\nabla \, u^*) \circ \widetilde{w}^\varepsilon \ - \ \nabla \, u^*\|_{L^2(\Omega)^n} \ \leq \ \varepsilon \|u^*\|_{W^{2,\infty}(\Omega)} \| \ \chi \ \|_{L^2(\Omega)^n}$$

which gives the desired result. ∎

5 Numerical results

In this section, we experimentally study the convergence and the accuracy of our multiscale method through numerical computations. For the sake of comparison we first implemented the method of T. Hou and X.-H. Wu [11], based on the direct numerical computation of the base functions defined in (27). We checked that our multiscale method in the $\mathbb{P}_1$ case, which is theoretically equivalent to the method of T. Hou and X.-H. Wu, does indeed coincide numerically although the implementations are quite different. The main novelty is the implementation of our $\mathbb{P}_2$ multiscale method (denoted by $\mathbb{P}_2$-MSFEM). As can be expected from the error estimate (28), its numerical results give a better approximation than the $\mathbb{P}_1$ method.

We first conduct numerical experiments in the periodic setting with a smooth scalar conductivity tensor (taken from [11])

$$A^\varepsilon(x) \ = \ a(x/\varepsilon) \, Id$$

where

$$a(x/\varepsilon) \ = \ 1/(2 + P \sin(2\pi x_1/\varepsilon))(2 + P \sin(2\pi x_2/\varepsilon)).$$

In this formula, P is used as a contrast parameter ($P = 1.8$ for the numerical results presented here). The right hand side of the Dirichlet boundary value problem is $f = -1$. All computations are performed on the unit square domain Ω which is uniformly meshed by triangular finite

elements (the coarse mesh of size h). Each triangle in this coarse mesh is again meshed by triangular finite elements (the local fine mesh of size $h' << h$). To make comparisons, we computed a reference solution (hopefully converged) on a very fine mesh of 10^6 degrees of freedom, with a classical $\mathbb{P}_1$-finite element method (denoted by $\mathbb{P}_1$-FEM). We also compared our solution to the approximate one given by the first two terms of the two-scale asymptotic expansion. The homogenized conductivity is given by $A^* = 1/2(4 - P^2)^{1/2}$.

Secondly, since the main interest of numerical homogenization is to compute approximate solutions in a non-periodic setting, we consider an heterogeneous composite material made of a pseudo random distribution of spherical inclusions in a background matrix. In such a case, there is of course no reference solution.

Let us recall once more that we are interested in the case $h > \varepsilon$ since the opposite case $h < \epsilon$ is covered by the classical finite element method in a much better way.

5.1 Periodic setting

Comparison with the two-scale asymptotic expansion A first obvious comparison is made between the two-scale asymptotic expansion and the $\mathbb{P}_2$-multiscale finite element approximation. This latter solution is computed on a coarse mesh with $h = 2 * 10^{-1}$ and a fine mesh $h' = 4 * 10^{-3}$. The asymptotic expansion (denoted by $\mathbb{P}_1$-FEM AE) is built from $\mathbb{P}_1$ finite element approximations of the homogenized solution and of the oscillating functions (see (2)). These latter ones are computed on the unit cell $Y = (0, 1)^2$ with periodic boundary conditions (see (3)). Figure 1 shows as expected a good approximation.

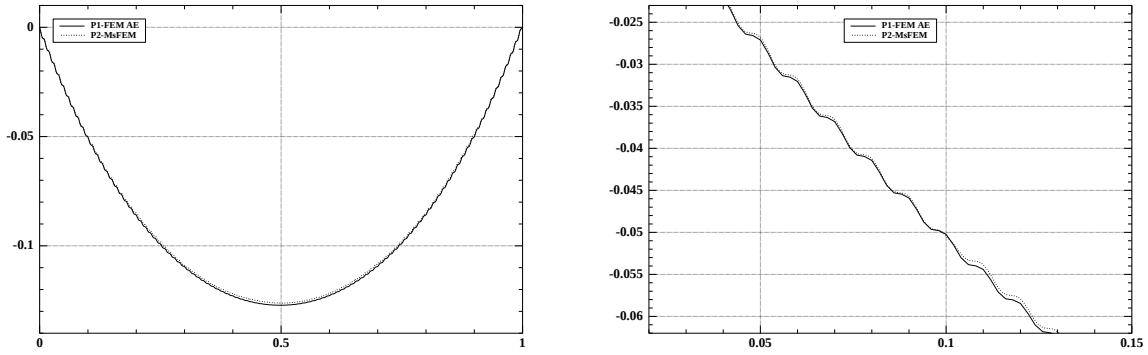

Figure 1: Cross-sections at $y = 0.5$ of the rebuilt solution from asymptotic expansion and multiscale approximation (left) with a close-up (right) : $\varepsilon = 10^{-2}$, $h = 1/5$ and $h' = h/500$.

Resonance effects and optimal mesh scale As we saw in the previous section, the theoretical bound of *the speed of convergence* of the method takes the form, for $k = 2$, $k' = 1$ and $h' = \frac{h}{M}$ (with $M = 500$ in our experiments)

$$g^\varepsilon(h) \;=\; h^2 + \sqrt{\frac{\varepsilon}{h}} + \frac{h}{M\varepsilon}.$$

Although $g^\varepsilon(h)$ is only an upper bound of the true error, it indicates that there exists an optimal $h^*(\varepsilon)$ mesh size (which depends on k too) such that the numerical error, or at least g^ε, is minimum. If we assume that M is very large, the order of this optimal value is

$$h^*(\varepsilon) \;\simeq\; \varepsilon^{1/5}. \tag{37}$$

According to [11] the resonance effect is the occurrence of large errors when the grid size h and the heterogeneities scale ϵ are close. This effect is also predicted by the above formula and is inherent to the multiscale framework used to compute the oscillating functions : the decomposition of the initial boundary value problems into independent smaller boundary value problems set on the coarse mesh element is somehow arbitrary.

The theoretical bound of the order of convergence, $g^\varepsilon(h)$, is not small when the discretization step h is close to ε (which is supposed to be very small). Therefore it is not a good idea to take h too small. Rather, in view of (37), the optimal discretization step $h^*(\varepsilon)$ is larger than ϵ. This is indeed confirmed by our numerical experiments shown on figure 2 where one can see that the behavior of the true numerical error (right) is close to that of the upper bound $g^\varepsilon(h)$ (left). It clearly indicates that there exists an optimal mesh size h^* (larger than ϵ) which minimizes the numerical error.

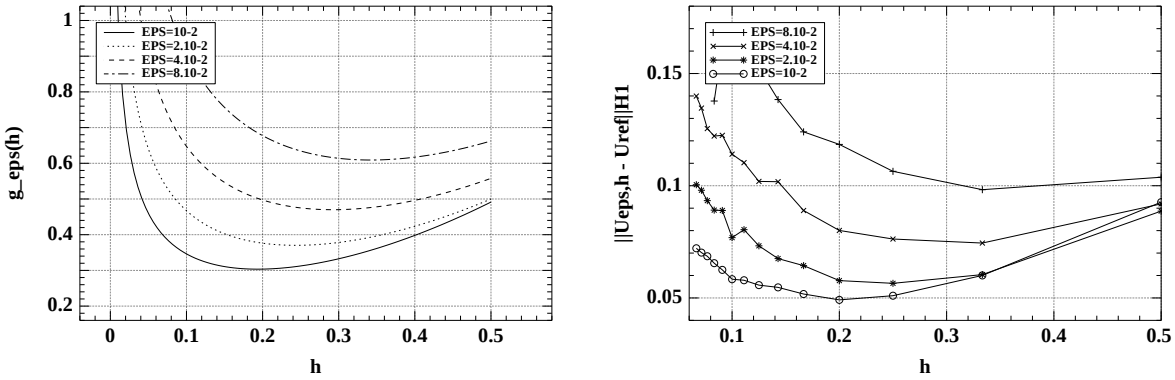

Figure 2: Predicted (left) and computed (right) error estimate as a function of h for different values of ε.

Convergence toward the homogenized solution We fix the ratio $M = h/h'$ (equal to 500) large enough so that $M > \varepsilon^{-1}$. Then, for different values of ϵ and for the optimal mesh size $h^*(\varepsilon)$ we compute the $\mathbb{P}_2$-MSFEM approximation of u^ε. One can check on figure 3 that this numerical approximation of u^ε clearly converges toward the homogenized solution.

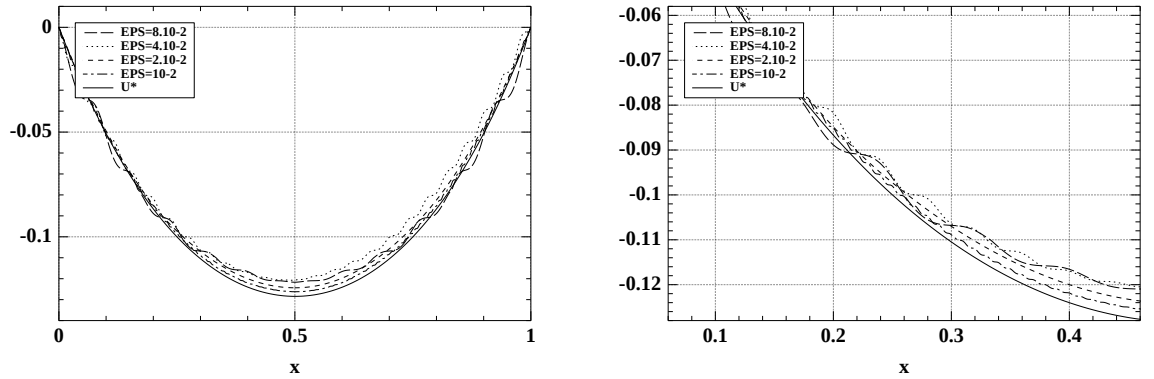

Figure 3: Convergence toward the homogenized solution for experimental h^* with $\varepsilon = 8.10^{-2}$, 4.10^{-2}, 2.10^{-2}, 10^{-2}: cross-section at $y = 0.5$ (left), and close-up (right).

Effects of the boundary conditions for the oscillating functions Imposing Dirichlet boundary conditions for the oscillating functions on each element K is a convenient, albeit arbitrary, choice. As a matter of fact it is one of the main problems of the method. Since the oscillating function $w^{\varepsilon,h}(x)$ is equal to the identity x on all boundary nodes on ∂K, see (22), it can not oscillate on theses boundaries. Therefore our multiscale method cannot mimic the oscillating properties of the true solution locally on the boundaries of the coarse mesh cells K. This effect is easily seen when we consider cross-sections of the solution along the sides of the elements of the coarse mesh (see figure 4).

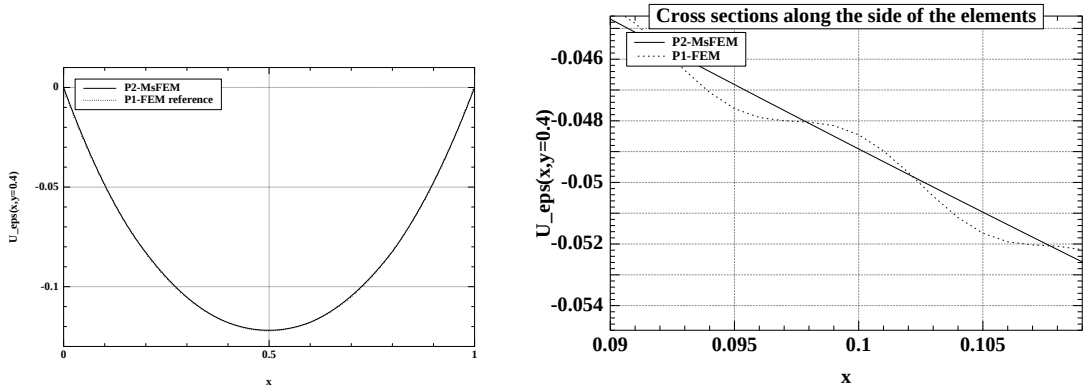

Figure 4: Cross-section (left) and close-up (right) at $y = 0.4$ of the reference and multiscale solutions: $\varepsilon = 10^{-2}, h^* = 1/5$.

On the other hand, the oscillating behavior of the solution is well captured inside the coarse mesh elements where the oscillations of the oscillating function $w^{\varepsilon,h}(x)$ are fully developed. The cross-sections of figure 5 show a very good approximation of the solution.

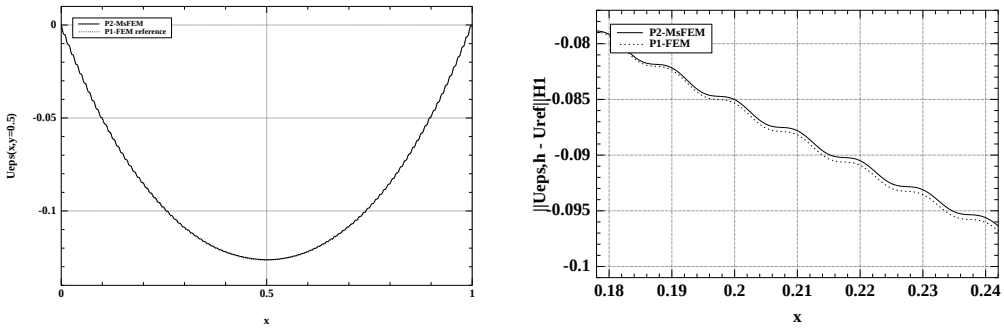

Figure 5: Cross section (left) and close-up (right) at $y = 0.5$ of the reference and multiscale solutions: $\varepsilon = 10^{-2}, h^* = 1/5$.

Very often in the literature, comparisons are made only on the value of the unknown u^ϵ and not on the values of its partial derivatives. In the periodic setting, the asymptotic expansion (2) shows that this comparison is too naive and simple because the corrector term is of order ϵ which is precisely small. A good comparison just implies that the homogenized solution is well captured. On the other hand, the gradient asymptotic expansion (3) shows that the corrector term is of order 1 for the partial derivatives. Thus, a good comparison of the gradient implies that, not only the homogenized solution is well captured, but also the local fluctuations due to the corrector term. It is therefore very important, in the periodic setting at least, to make precise comparisons for the gradient field $\mathrm{grad} u^\epsilon$ or the flux $A^\epsilon \mathrm{grad} u^\epsilon$. This is done on figures 6 and 7 where we see a remarkably good agreement, except at those nodes located at the coarse

cell boundaries. As already explained, this last effect is due to the applied affine boundary conditions for the oscillating functions $w^{\varepsilon,h}$. Indeed, the overshoots and undershoots on figures 6 and 7 take place precisely at the interface between two coarse mesh elements.

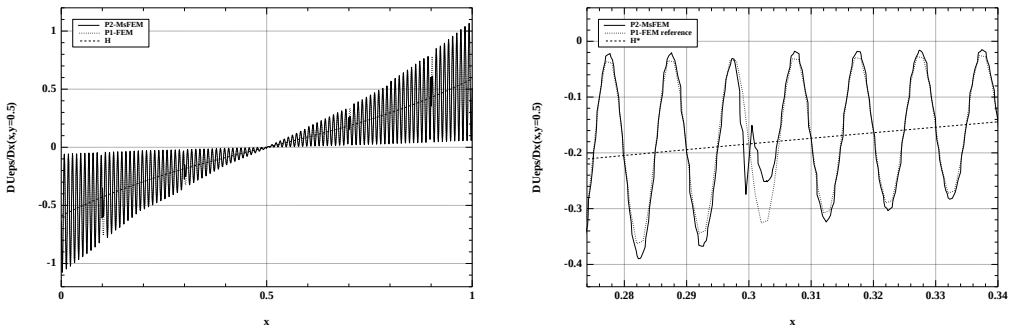

Figure 6: Cross-section (left) and close-up (right) of the partial derivative $\partial U^\varepsilon/\partial x$ at $y = 0.5$ of the reference and multiscale solutions: $\varepsilon = 10^{-2}, h^* = 1/5$. Here, H stands for the homogenized solution.

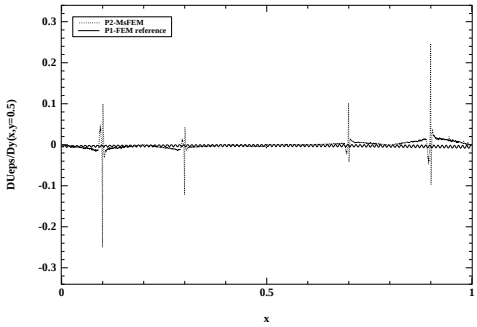

Figure 7: Cross-section of the partial derivative $\partial U^\varepsilon/\partial y$ at $y = 0.5$ of the reference and multiscale solutions: $\varepsilon = 10^{-2}, h^* = 1/5$.

5.2 Two-phase composite material

Our multiscale finite element method is not designed for periodic homogenization but rather for general numerical homogenization when no explicit asymptotic expansion of the solution is known. As a model problem we consider the study of the conductivity properties (or anti-plane elasticity properties) of a two-phase composite material made of spherical inclusions in a background matrix. Both phases are isotropic with a high conductivity $a^\epsilon(x) = 100$ in the inclusions and a lower one $a^\varepsilon(x) = 1$ in the matrix. The inclusions are randomly distributed in the computational domain $\Omega = (0,1)^2$. On purpose we choose a large number of 10^6 inclusions so that a direct computation is out of reach with a standard finite element method. This numerical experiment corresponds to a minimum distance between two inclusions of $\varepsilon = 8 * 10^{-4}$ and a particle diameter of $\varepsilon/2$.

The right hand side of the elliptic boundary value problem is equal to zero and the solution satisfies mixed boundary conditions :

- Dirichlet ones on the sides denoted by Γ_0 ($u_\varepsilon = 0$ on lower side and $u^\varepsilon = 1$ on the upper one),

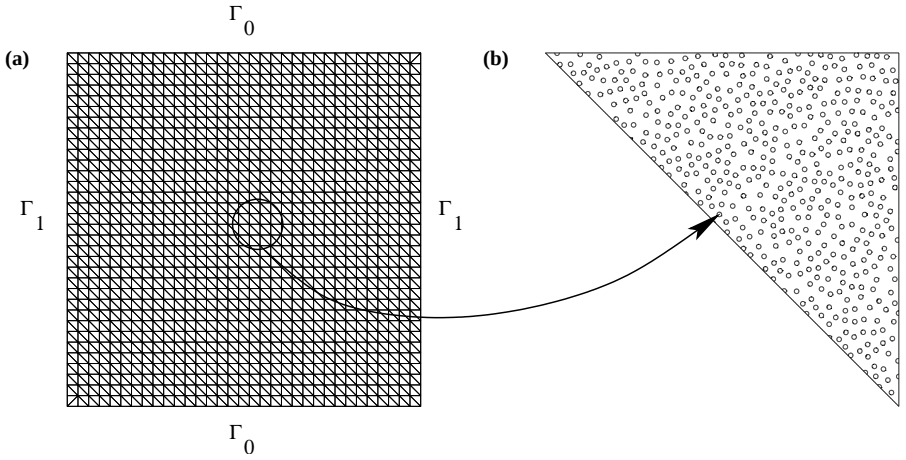

Figure 8: (a) The coarse mesh of $\Omega = (0,1)^2$, (b) Close-up on the inclusions: $h = 1/33$ and $h' = h/500$.

- Homogeneous Neumann ones take place on the left and right sides denoted by Γ_1 ($a^\varepsilon \text{grad}\, u^\varepsilon \cdot n = 0$ where n is the normal unit vector to $\partial\Omega$).

Figure 8 shows the approximated $\mathbb{P}_2$-MSFEM solution u^ε into a coarse element. It varies almost linearly as the homogenized solution. As noticed before, a much more interesting numerical result is the profile of the flux field $a^\varepsilon \text{grad}\, u^\varepsilon$.

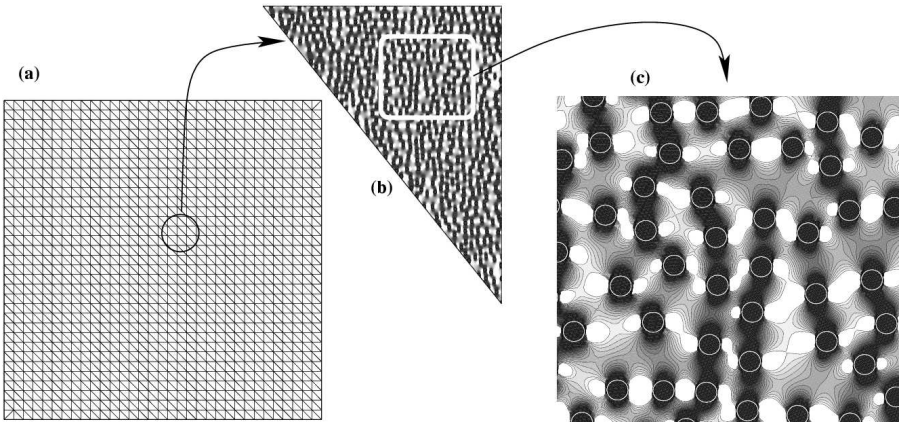

Figure 9: (a) The coarse mesh, (b) Flux density i.e. $\|a^\varepsilon \text{grad}\, u^\varepsilon\|_{\mathbb{R}^2}$ in an element of the coarse mesh and (c) a close-up.

As already explained, the affine boundary conditions for the oscillating functions breaks their necessary oscillating character on the coarse cell boundaries. This generates localized large errors for the gradient at those boundaries (see figures 6 and 7). In the present case, since the conductivity jumps between the two phases, the errors are unacceptably large. Therefore, in order to circumvent this difficulty, we implemented another kind of boundary conditions which gives a better approximation. Following an idea of [11] we solve 1-d elliptic problems on each line line segment of ∂K and these 1-d solutions are used as boundary conditions for the oscillating functions $w^{\varepsilon,h}$. The boundary conditions for those 1-d problems are of Dirichlet type: the nodal values at the corners of K must be equal to x. In numerical practice, we approximate the value of the oscillating functions on each side of ∂K by piecewise linear functions. The inclusions which intersect the sides of this element generate a partition composed of segments.

If s denotes the curvilinear coordinate on the coarse element boundary, on each segment we take $w_i^{\varepsilon,K} = ps + q \,\text{on}\, \partial K$ where p and q are constants. At the ends of two contiguous segments, we write the conditions of continuity of the functions and of the tangential derivatives (i.e. along the boundary of the element). This last condition is true only if the normal unit vector to ∂K coincide with the unit vector supported by the side of the element.

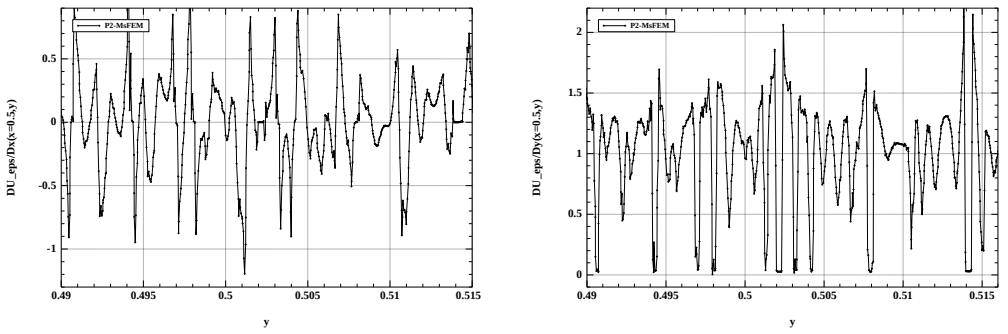

Figure 10: Close-up of the cross-sections of the partial derivatives $\partial U^\varepsilon/\partial x(x = 0.5, y)$ and $\partial U^\varepsilon/\partial y(x = 0.5, y)$ of the multiscale solution : $\varepsilon = 8 * 10^{-4}, h^* = 1/33$.

This modification of the boundary conditions for the oscillating functions $w^{\varepsilon,h}$ greatly improves the precision of the multiscale finite element method at the interface betweens two coarse mesh cells. For example, figure 9 displays the norm of the flux vector. At a very small scale, one can clearly see the diffusion channels between close inclusions. This proves that our method is able to reproduce the fine details of the local fluctuations.

Acknowledgments. The work of both authors has been supported by the GdR MoMaS CNRS-2439 sponsored by ANDRA, BRGM, CEA and EDF whose support is gratefully acknowledged.

References

[1] G. ALESSANDRINI, V. NESI, *Univalent σ-harmonic mappings,* Arch. Ration. Mech. Anal. 158, 155–171 (2001).

[2] G. ALLAIRE, *Shape Optimization by the homogenization method*, Applied Mathematical Sciences, 146, Springer, (2002).

[3] T. ARBOGAST, *Numerical subgrid upscaling of two-phase flow in porous media,* in Numerical treatment of multiphase flows in porous media, Lecture Notes in Physics, vol. 552, Chen, Ewing and Shi eds., pp.35-49 (2000).

[4] I. BABUSKA, *Solution of interface problems by homogenization I, II, III*, SIAM J. Math. Anal. **7**, pp. 603–634, pp. 635-645 (1976) and **8**, pp. 923-937 (1977).

[5] A. BENSOUSSAN, J.L. LIONS and G. PAPANICOLAOU, *Asymptotic analysis for periodic structures*, Studies in Mathematics and its applications, Vol. 5, North-Holland Publishing company, (1978).

[6] Y. CAPDEBOSCQ, M. VOGELIUS, *Wavelet Based Homogenization of a 2 Dimensional Elliptic Problem,* to appear.

[7] P. CIARLET, *The finite element methods for elliptic problems,* North-Holland, Amsterdam (1978).

[8] W. E, B. ENGQUIST, *The heterogeneous multiscale methods,* Commun. Math. Sci. 1, 87–132 (2003).

[9] Y. EFENDIEV, T. HOU, X.-H. WU, *Convergence of a nonconforming multiscale finite element method,* SIAM J. Numer. Anal. 37, 888–910 (2000).

[10] Y. EFENDIEV, X.-H. WU, *Multiscale finite element methods for problems with highly oscillatory coefficients,* Numerische Math., vol.90(3), 459-486 (2002).

[11] T. Y. HOU, X.-H. WU, *A multiscale finite element method for elliptic problems in composite materials and porous media*, Journal of computational physics 134, 169-189, (1997).

[12] T. Y. HOU, X.-H. WU, Z. CAI, *Convergence of a multiscale finite element method for elliptic problems with rapidly oscillating coefficients*, Math. of Comp. 68, 913-943, (1999).

[13] A.-M. MATACHE, I. BABUSKA, C. SCHWAB, *Generalized p-FEM in homogenization,* Numer. Math. 86, 319–375 (2000).

[14] A.-M. MATACHE, C. SCHWAB, *Two-scale FEM for homogenization problems,* M2AN Math. Model. Numer. Anal. 36, 537–572 (2002).

[15] F. MURAT, L. TARTAR, *H-convergence*, in Topics in the mathematical modeling of composite materials, A. Cherkaev and R.V. Kohn eds., series : Progress in Nonlinear Differential Equations and their Applications, Birkhaüser, Boston 1997. French version : mimeographed notes, séminaire d'Analyse Fonctionnelle et Numérique de l'Université d'Alger (1978).

[16] P. H. RABINOWITZ, *Théorie du degré topologique et applications à des problèmes aux limites non linéaires*, rédigé par H. BERESTYCKI, Publications du Laboratoire d'Analyse Numérique, Université de Paris VI, 4, place Jussieu, Paris, N^o 75010.